Biochimica et Biophysica Acta, 406 (1975) 329–346

BBA 77081

A THEORETICAL MODEL FOR LIPID MONOLAYER PHASE TRANSITIONS

H. L. SCOTT, Jr

Department of Physics, Oklahoma State University, Stillwater, Okla. 74074 (U.S.A.)

(Received April 1st, 1975)

SUMMARY

We present a theoretical model for the liquid-expanded to liquid-condensed phase transition observed in many phospholipid monolayer films. The total two-dimensional pressure in the model is the sum of the hydrocarbon chain pressure and the surface pressure. The hydrocarbon chain pressure is calculated in an extended version of a model published earlier. The surface pressure results from a lowering of the surface tension in the monolayer over that of pure water, thus producing a force on a Langmuir float. When these two contributions are added, π/A isotherms are obtained which have slope discontinuities very similar to those observed experimentally. These results indicate that a successful model for lipid phase behavior must consider the interactions between head groups and water as well as cooperative hydrocarbon chain melting.

(I) INTRODUCTION

The pressure vs area isotherms of phospholipid monolayers spread on an air-water interface [1] offer alternative means to the analysis of bilayer or micellar structures in solution for the studies of the effects of lipid-lipid and lipid-water interactions. Monolayer experiments provide a direct control over the molecular arrangement so that an experimenter may make use of the independent variables temperature and area (or surface pressure). In experiments with dispersions, an experimenter may vary temperature or concentration, and concentration differences mainly affect the size and shape of the structures formed by lipids in water [2]. Thus, a great many studies have been made of films of fatty acids [3]. A general review of monolayer properties and experimental methods is given by Gaines [4].

Experiments involving monolayer films of phospholipids have received considerable attention [1] as possible sources of information on lipid behavior in bilayer membranes. When sufficiently pure phospholipid monolayers are spread at an air-water interface measured isotherms, below some critical temperature, have "kinks" or slope discontinuities at surface areas which are larger at lower temperatures. Phillips and Chapman [1] interpret these discontinuities as signalling the onset of phase transitions between "liquid expanded" and "liquid condensed" phases, much as simple liquid vapor isotherms below the critical temperature have slope discontinuities

signalling entry into the two phase region. The major difference between simple fluid transitions and the phospholipid monolayer transitions lies in the slope of the isotherms in the two phase region. For simple fluids this slope is zero (i.e. the isotherms are flat) while relatively condensed monolayer experiments seem to show, in most cases, that surface pressure π rises with decreasing surface area A even in the two phase region. In both lipid monolayers and simple fluids, phase transitions apparently disappear for temperatures above a certain critical value. Lipid monolayers also show, at low pressures and large surface areas (approx. 200 $Å^2$) a phase transition from the liquid expanded state to a gaseous state with surface areas of several thousand square angstroms [5]. In this transition the isotherms do, in fact, have flat portions in the two phase region.

Recently a rigorous theoretical attempt to describe hydrocarbon chain thermodynamics was performed by Nagle [6]. Nagle [6] treated steric interactions within a line of long chains exactly, and approximately included van der Waals attractive forces. The model in its original form provided a description of the melting-type phase transition in lipid-water dispersions which occurs at one temperature only (for sufficiently high lipid concentrations). Nagle [7] has recently adapted his model to the monolayer problem through introduction of a surface area A, defined in terms of pre-existing parameters in the model, and the thermodynamic conjugate variable to A, the surface pressure π. In the model, Nagle [7] finds π/A isotherms which have flat portions in the two phase region below the critical temperature. Nagle's [7] model is most useful for its exact treatment of the steric chain repulsions. The model shows that theoretically, one expects cooperative chain behavior to be the primary cause of the observed anomalous thermal behavior in lipid-water systems.

A second theoretical model for monolayer liquid expanded-condensed phase transitions has been proposed by Marčelja [8]. In this model the energies of each of the possible conformational states of a single chain are calculated in the average force field of the neighboring chains. The accuracy of this technique was proven in an application to the even-odd effect in liquid crystals with CH_2 end chains [9]. This was the first theoretical model to reproduce the oscillation of transition temperature through the $(CH_2)_n$ series of end chains. In the application of this model to the monolayer problem, Marčelja [8] includes steric forces, previously neglected, by introducing an external surface pressure π which has the effect of limiting the available surface area. This in turn limits the available states for the hydrocarbon chains, since an area is associated with each state. The resulting isotherms Marčelja [8] produces are in remarkable agreement with experiment, although flat isotherms are again produced.

The reasons for this discrepancy in the shapes of the experimental and theoretical isotherms in the two phase region is not known. It is possible that impurities in the surface monolayer region disrupt the cooperativity of the hydrocarbon chains and thereby produce the rounded isotherms observed experimentally [8]. However, impurities do not seem to affect the liquid-expanded gas transition observed at lower pressures in the same systems [5]. Another possible source of the rounding of the experimental isotherms is the contribution to the surface pressure of the polar head groups located in the water surface itself. The theoretical calculation of Marčelja does not consider this effect, although estimates made at large areas per molecule [2] indicate that the repulsive energy of the polar head groups is a strongly varying function of area/molecule.

The purpose of this paper is 2-fold. Firstly, we wish to present the results of a new version of an earlier model for monolayer phase transitions [10] which decreases earlier discrepancies with experiments. Secondly, we describe a calculation which estimates the contribution to the surface pressure of the head group-water interactions. We will show that, upon combining the contributions to π from the hydrocarbon chains and the head groups, isotherms may be derived which have the qualitative shapes which are in agreement with experiment.

In Section II we describe the model for the hydrocarbon chains and the resulting π/A isotherms for chains only. In Section III we present an estimate of the contribution to π due to a reduction in surface tension of the water-head group monolayer relative to a pure water surface. The results of this calculation are then combined with the results of the preceding section to produce π/A isotherms which we compare with experiment. Section IV contains our conclusions.

(II) THE HYDROCARBON CHAIN MODEL

The model we use for the hydrocarbon chain phase transition is the subject of an earlier paper [10]. For a detailed description of the computational techniques the reader is referred to this work. Here, we describe the basic features of the model and the improvements that have been made.

The model is constructed in the following fashion. The two-dimensional region of finite thickness in which the chains lie is divided into a number of two-dimensional layers. The number of layers is equal to the number of CH_2 groups in a chain so that, when the chain is in the all-*trans* state, one CH_2 per chain lies in each layer. Then within each layer the volume is partitioned into cells. The cell size is chosen so that one CH_2 group only may fit into a cell. The steric portion of the hydrocarbon chain interactions then is equivalent to the criterion that only one CH_2 may occupy a given cell at any instant. To incorporate isomeric disorder into the model the chains are allowed to zig-zag and fold. In this way one may construct different chain conformations by drawing different patterns for the occupation of cells in the various layers. The states of the model to be discussed in this paper are shown in Fig. 1. The model is 15 layers thick, and each molecule has two chains of 15 units each. State 0 represents the all-*trans* conformation. States 1 through 9 depict the shapes of the molecules if one gauche rotation occurs at various locations on one of the chains. Molecules in states 10 and 11 have a gauche rotation at a lower position in each chain. States 12 through 20 represent "kink" states of the type proposed by Seelig [11] in which a series of three C-C bonds adopt a gauche-*trans*-gauche conformation to produce the shapes shown.

There are, of course, many more than 20 possible conformations of 15 unit chains (we consider only 12 of these units as rotatable, excluding the last unit and the top two). To partially compensate for not explicitly including all possible states we have assigned weights W_i to each of the states according to Table I. The weights for the kink states are large because, if the kink is allowed to fluctuate up and down a chain [11] then a simple counting shows there are 12 ways to place one kink, 55 ways to place two kinks, 120 ways to place three kinks, 126 ways to place four kinks, and 49 ways to place five kinks on the chain. If we use these values then, for example, state 17, which has two kinks, may be formed in $12 \times 12 + 2(55) = 254$ ways, since one may have either both kinks on one chain or one kink on each chain.

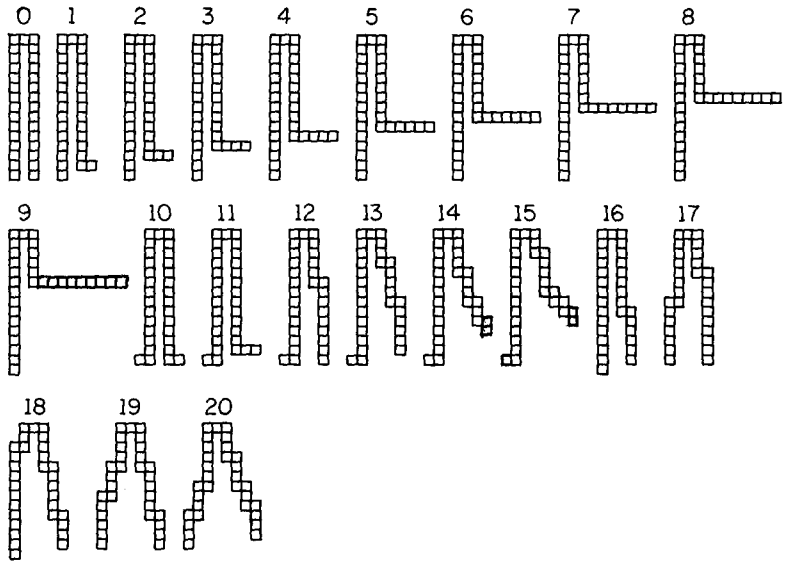

Fig. 1. The 21 molecular states allowed in the model. State 0 is the all-*trans* state. States 1–9 involve a single gauche rotation. States 10 and 11 involve two gauche rotations. States 12–20 all involve one or more kinks which can occur at any point in either chain in a molecule. In the calculations this means that kink states effectively require the molecule to occupy an entire extra vertical column per kink.

TABLE I

WEIGHTS FOR THE STATES OF FIG. 1

State	0	2–9	10	11	12	13	14	15	16	17	18	19	20
Weight	1	2	1	2	46	374	2698	9998	24	254	1560	6157	16 322

The computations proceed as follows [10]: For a given density ρ and temperature T we calculate the Helmholtz free energy of the model for a given set of chain configurations for the molecules. That is, if we let α_i denote the fraction of molecules in state i then for given $\{\alpha_i\}$, ρ, and T we calculate F. Then the values of the α_i which are found at thermodynamic equilibrium are these for which F is a minimum. The free energy is calculated by first approximately calculating the entropy for a given ρ and $\{\alpha_i\}_{i=0}^{20}$. The method employed here is based on a modification [12, 13] of a technique due to Flory [14]. As pointed out by Nagle [15], the approximate technique cannot be expected to perfectly reproduce the properties of exactly soluble models, since cyclic or loop correlations are neglected. However, aside from exactly soluble models [6, 7] which are in several ways oversimplified in order to make the extremely difficult mathematical analysis possible, the model presented here seems to be the only plausible way so far to consider seriously the hardcore forces in the CH_2 chains in a model which appears more realistic. Also, Straley [16] has pointed out that Alben's method [12, 13] agrees well with Onsager's [17] exact virial expansion for long rods.

Thus, in our calculation, where the chains are long but not rigid we might expect to at least qualitatively reproduce the properties of phospholipid layers.

After the entropy is calculated by the above technique the energy is computed in the following fashion. The first contribution to the energy is the excitation energies for the individual isomeric states. To this end we assign an energy $\varepsilon = 500$ cal/mol for each gauche rotation [10]. Thus, for example, state 1 contributes energy $N\alpha_1\varepsilon$ to the total, and state 20 contributes energy $N\alpha_{20}$ (10ε) since each kink in this state involves two gauche rotations. Recall the α_i represent the fraction of molecules in the ith state. The other contribution to the internal energy comes from the van der Waals attractive forces. As in ref. 10 we take this term to be of the form

$$-A\rho^{\frac{3}{2}} \tag{1}$$

where A is a constant and the power $\frac{3}{2}$ results from a $1/r^5$ attractive energy which is integrated over the entire two-dimensional layer. The presence of an attractive energy is necessary in order that the model exhibit phase transitions. Following the procedure of ref. 10 we find the thermodynamic functions of the model to be

$$\begin{aligned} S/Nk = {} & 1-\sum_{i=0}^{20}\alpha_i \ln \alpha_i+\sum_{i=0}^{20}W_i \ln \alpha_i \\ & +f(\rho X_0)(3+\alpha_{12}+2\alpha_{13}+3\alpha_{14}+4\alpha_{15}+\alpha_{16}+2\alpha_{17}+3\alpha_{18}+4\alpha_{19}+5\alpha_{20}) \\ & +f(\rho X_1)(\alpha_1+2\alpha_{10}+\alpha_{11}+\alpha_{12}+\alpha_{13}+\alpha_{14}+\alpha_{15})+2f(\rho X_2)(\alpha_2+\alpha_{11}) \\ & +3\alpha_3 f(\rho X_3)+4\alpha_4 f(\rho X_4)+5\alpha_5 f(\rho X_5)+6\alpha_6 f(\rho X_6)+7\alpha_7 f(\rho X_7)+8\alpha_8 f(\rho X_8) \\ & +9\alpha_9 f(\rho X_9) \end{aligned} \tag{2}$$

$$\begin{aligned} E = {} & -A\rho^{\frac{3}{2}}+\sum_{i=1}^{9}\alpha_i\varepsilon_i+2\varepsilon(\alpha_{10}+\alpha_{11})+3\varepsilon\alpha_{12}+5\varepsilon\alpha_{13}+7\varepsilon\alpha_{14} \\ & +9\varepsilon\alpha_{15}+2\varepsilon\alpha_{16}+4\varepsilon\alpha_{17}+6\varepsilon\alpha_{18}+8\varepsilon\alpha_{19}+10\varepsilon\alpha_{20} \end{aligned} \tag{3}$$

$$F = E-TS \tag{4}$$

where

$$f(y) = -\frac{1}{y}[(1-y)\ln(1-y)+y] \tag{5}$$

and the functionals X_0–X_9 are linear functions of the $\{\alpha_1\}$ which are listed in Appendix A. The values of α_i which minimize F, Eqn. 4, are found numerically by solving the 20×20 system of non-linear algebraic equations which arise upon differentiation of Eqns 2 and 3.

The two adjustable parameters in this model are the excitation energy ε and the van der Waals interaction strength A. In this paper we fix $\varepsilon = 500$ cal/mol [10] and we fix T in each numerical run. Then the value of A used is that value for which the phase transition begins at area A_e in the expanded phase which is consistent with the experimental area of this phase for the given T. This procedure is different from that of ref. 10. In the previous paper, the ratio A/ε was treated as the adjustable parameter. The experimental check on the value of A is the heat of sublimation which should roughly measure the total cohesive energy of the system. For the n-alkaline homologs, this value is 1.84 kcal/mol CH_2 [6]. However, for condensed monolayers Gershfeld

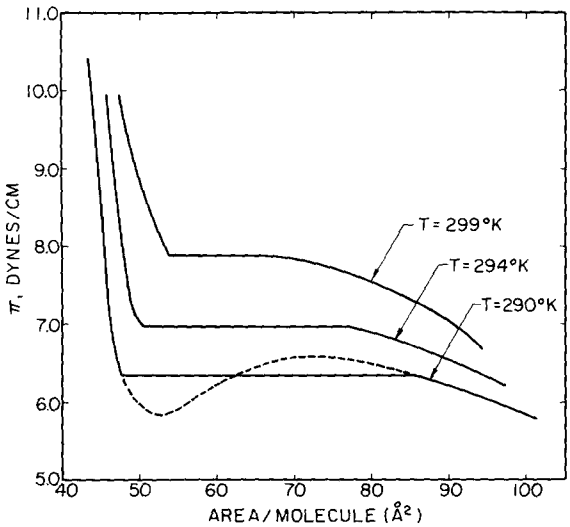

Fig. 2. Theoretical π/A isotherms for the hydrocarbon chain models for $T = 290$, 294, and 299 °K. The van der Waals loops which occur in the numerical analysis are shown in the $T = 290$ °K isotherm.

[18] has found cohesive energies of only 100–400 cal/mol CH_2, considerably less than the value for paraffins.

In Fig. 2 we show π/A isotherm for the hydrocarbon chains for three temperatures, 290, 294, and 299 °K. The isotherms are characterized by van der Waals loops which are replaced by horizontal lines according to the Maxwell Equal Area rule, equivalent to minimizing the free energy in the two phase region. Examination of these isotherms shows that the surface areas per molecule at the condensed phase end of the transitions are different from experimental values. Also, the pressures are generally too low. The condensed phase area disagreement may not be serious. It is very difficult to estimate this quantity from the experiments, and Phillips and Chapman [1] assume a single value for all temperatures, which is nearly the close-packed area per molecule. There is no slope discontinuity at the high pressure end of the transition to unambiguously locate the point in question. In the next section we shall give theoretical arguments for the existence of this point, although the associated slope discontinuity will be shown to be so slight as to be nearly unobservable. The discrepancy in pressure is probably in part a defect of the model, but it is also, we believe, partially due to the fact that we have ignored the head group contributions to π so far. The parameter Λ was adjusted in the calculations for $T = 290$, $T = 294$, and $T = 299$ °K so that Λ/RT assumed the values 29, 28.6, and 28.1, respectively. The value of the van der Waals constant determined from these values is 8400 cal/mol within ± 10 cal/mol for each value of Λ/RT so that it is actually necessary only to assign a value to this parameter at one temperature and isotherms at nearby temperatures will also be correct. In this case, because of the large number of CH_2 groups per molecule the values of Λ yield cohesive energies smaller than the experimental 1.84 kcal/mol CH_2 but in good agreement with the values obtained by Gershfeld [18].

In Fig. 3 we show, for $T = 290$ °K, plots of the isomeric disorder (the α_i in

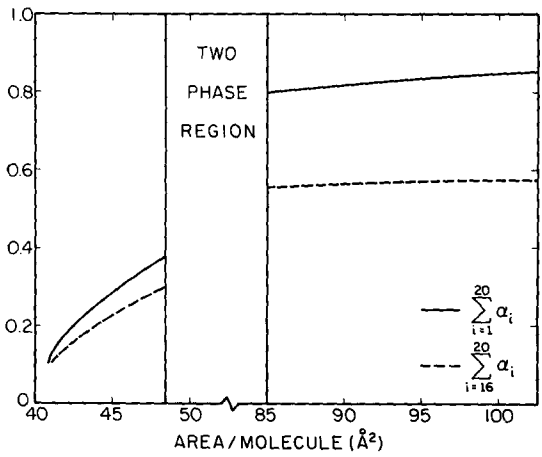

Fig. 3. A plot of the isomeric disorder in the model as a function of molecular area for $T = 290$ °K. The solid line represents the total disorder, i.e. the fraction of all molecules not in state 0. The dashed line represents the fraction of all molecules in the pure kink states (16–20). The kink states make up a substantial portion of the total disorder at all areas. In the two phase region, the total disorder fluctuates between the two extremes on either side. Note that the condensed phase is not completely all-*trans* in this model and most of the disorder consists of kink states.

this model) versus surface area per molecule. Due to the large number of order parameters we have plotted only the disorder in kink states and the total disorder. The model here confirms the hypothesis of Seelig [11] that kink states seem to dominate over other isomeric states in the neighborhood of the transitions especially in the condensed phase. This is purely a result of steric interactions in this model. We turn now to a calculation of the head group-water contribution to the surface pressure.

(III) SURFACE PRESSURE OF THE HEAD GROUP-WATER MIXTURE

In a Langmuir film balance experiment one generally measures as surface pressure the reduction in substrate surface tension on one side of a float due to the presence of the film. In the case under consideration here, in which the film consists of phospholipids, the head groups interact rather strongly with the water substrate. Thus, any theory which attempts to explain monolayer phase behavior must, it seems, consider this aspect of the problem as well as the effect of the hydrocarbon chains considered in the previous section.

Due to the complicated nature of the head groups and the lack of information concerning the physical state of the water near the head groups we will take the following approach. First, we make use of an equation due to Defay et al. [19] for surface pressure of the monolayer film of head groups. The equation, which closely resembles the formula for osmotic pressure across a semipermeable membrane, has the form

$$\pi = \sigma_0 - \sigma = -\frac{kT}{a} \ln x_s \gamma_{s,R} \tag{6}$$

when a is the area occupied by a single water molecule, $\boldsymbol{k}$ is Boltzmann's constant, σ is the surface tension of the monolayer, considered to be a two-dimensional solution of head groups and water, x_s is the concentration of substrate (water) in the monolayer, and $\gamma_{s,R}$ is the so-called activity coefficient [20] of the water in the surface measured relative to the activity coefficient of pure water. Thus, $\gamma_{s,R}$ is a measure of head group-water interactions. In Appendix B we give a derivation of Eqn 6.

In order to make use of Eqn. 6 we must find an expression for $\gamma_{s,R}$. In general, the activity coefficient is defined for a system by the departure of the chemical potential from its ideal value [20]:

$$\mu_i = \mu_i(\text{ideal}) + \boldsymbol{k}T \ln x_i \gamma_i \tag{7}$$

Thus, it should be possible, using statistical mechanics, to determine the manner in which the γ_i term depends upon interparticle forces. In Appendix C we derive the following general relation:

$$\ln x_i \gamma_i = -\partial / \partial N_i \ln q(N_{i1}, \ldots) \tag{8}$$

where

$$q(N_1, \ldots) = \frac{1}{V^N} \int \mathrm{d}\vec{r}_{11} \ldots \mathrm{d}\vec{r}_{N_1} \mathrm{d}\vec{r}_{12} \ldots \mathrm{d}\vec{r}_{N_2} \, \mathrm{e}^{-\beta U} \tag{9}$$

where $\beta = 1/\boldsymbol{k}T$, $\boldsymbol{k}$ is Boltzmann's constant, N_i is the number of particles of type i, and N is the total number of particles. The quantity U is the total intermolecular potential energy, a function in general of the coordinates of all the particles.

Now in order to estimate the surface pressure we must specify a model for which q_{N_1,N_2} can be evaluated. In a complex dipolar system involving relatively large polar head groups and relatively small polar water molecules precise statistical mechanical calculations are very difficult to perform. The picture is complicated even more by the fact that some water apparently binds to the polar head groups in the monolayer [21]. At sufficiently low temperatures (near 0 °C) it is probably safe to assume that dipolar forces are strongly shielded due to dipolar ordering so that we may, as a first approximation, consider the net effect of these forces on any one surface molecule to be a uniform electric field E. In order to properly take account for the different sizes of the free water molecules and the water-bound head groups we shall divide the surface monolayer into cells. Thus, we shall use a model in which molecules in the surface are confined to cells and experience a uniform electric field due to the net effect of ordered dipoles in the surface and subsurface layers. In a model of this type it is the unequal sizes of the two surface constituents which leads to a substantial lowering of surface tension, and thus to an estimate of the surface pressure.

We divide the surface up into M cells, each of which is the same size as the lipid head group plus its bound water. The bulk water is assumed to contribute only through the net molecular electric field, so we consider explicitly only the portion of q_N due to surface molecules. Since the area occupied by a typical lecithin head group is about 39–40 Å^2 [22] and the area occupied by water on the surface is about 9.6–10 Å^2 [23], we take the size of the lipid cells to be four times bigger than the water surface area. Then every cell which is not occupied by a lipid will contain four water molecules. If all surface particles are confined to cells and the dipole-dipole forces

combine to produce a uniform field then the configuration integral can be evaluated to give

$$q_{N_1;\,N_2} = \frac{a_1^{N_1} a_2^{N_2}}{A^{N_1+N_2}} (e^{-\beta u_1 E})^{N_1} (e^{-\beta u_2 E})^{N_2} \Omega(N_1, N_2), \tag{10}$$

where a_i and u_i represent the area per molecule and the dipole moment of a molecule of species i, and A is the total area of the monolayer. The quantity $\Omega(N_1,N_2)$, which arises naturally from evaluation of the $2N$-dimensional configuration integral within the cell model constraints, is the number of possible ways the molecules may be arranged in the cells. Now if there are M cells, N_w free (unbound) water molecules, and N_L lipids, then

$$M = N_L + N_w/4 \tag{11}$$

Furthermore, the total number of surface molecules is

$$N = N_L + N_w \tag{12}$$

The quantity $\Omega(N_L,N_w)$ is therefore simply

$$\Omega(N_L, N_w) = \binom{M}{N_L} = \frac{M!}{N_L!(M-N_L)!}, \tag{13}$$

the number of ways the N_L lipids can be arranged in the M cells. It is also worth noting that Eqn 13 assumes random placement of the polar head groups on the surface without regard to chain conformation. If we allow the head groups some mobility with respect to the chains, and if we confine the model in use to large area/molecule, then this approximation should not present any serious difficulties. Theoretical studies [24] do, in fact, indicate the head groups have some conformational freedom.

Now taking the logarithmic derivative of Eqn 10 with respect to N_w, (setting $N_1 = N_L$, $N_2 = N_w$)

$$-\partial/\partial N_w \ln q_{N_L, N_w} = (A - a_2 + \beta u_2 E) - \partial/\partial N_w \ln \Omega(N_L, N_w). \tag{14}$$

Therefore

$$\ln x_w \gamma_s = (A - a_2 + \beta u_2 E) - \partial/\partial N_w \ln \Omega(N_L, N_w) \tag{15}$$

But for the pure system, $x_w = 1$ and $\Omega(N_L,N_w) = 1$;

$$\ln \gamma_s(\text{pure}) = A - a_2 + \beta u_2 E. \tag{16}$$

Thus

$$\ln x_w \gamma_s - \ln \gamma_s(\text{pure}) = \ln x_w \gamma_{s,R} = -\partial/\partial N_w \ln \Omega(N_L, N_w). \tag{17}$$

Therefore, in this model the quantity $\Omega(N_L,N_w)$ gives rise to a non-zero surface pressure. Now we may use Stirling's Approximation for the factorial terms and perform the differentiation to obtain

$$\ln x_w \gamma_{s,R} = \tfrac{1}{4} \ln \frac{N_w/4}{N_L + N_w/4} \tag{18}$$

Now, using Eqn 12 to eliminate N_w in favor of N, in the denominator, the total number of molecules, we find

$$\ln x_w \gamma_{s,R} = \tfrac{1}{4} \ln \frac{N_w}{N + 3N_L} \tag{19}$$

or, in terms of the mole fractions, $x_w = N_w/N$ and $x_L = N_L/N$,

$$\ln x_w \gamma_{s,R} = \tfrac{1}{4} \ln \frac{x_w}{1 + 3x_L} \tag{20}$$

Now substituting into Eqn 6 for π we have

$$\pi = \frac{-kT}{4a} \ln \left(\frac{x_w}{1 + 3x_L} \right) \tag{21}$$

This relation for surface pressure is plotted in Fig. 4 (the dashed curve) for $T =$ 290 °K against area per lipid molecule.

Also, in Fig. 4 we plot for $T = 290$ and $T = 299$ °K, the isotherms for the total pressure in the monolayer due to chains and head groups. These plots are generated by adding the isotherms of Fig. 2 to the isotherms generated by Eqn 21. This procedure is valid only if the observed phase transition in monolayers is not an ideal isothermal first-order phase transition. When we add the two pressures separately, we

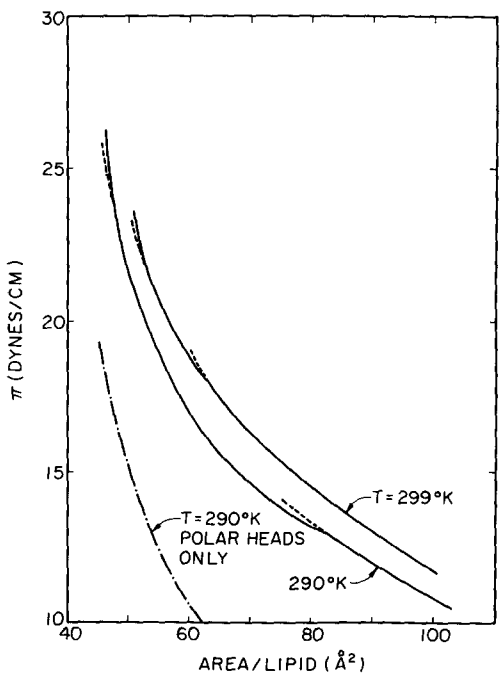

Fig. 4. π/A isotherms for $T = 290$ and 299 °K. The dashed line is the portion of the 290 °K isotherm from Eqn 21 only. The dotted segments illustrate the slope discontinuities in the isotherms.

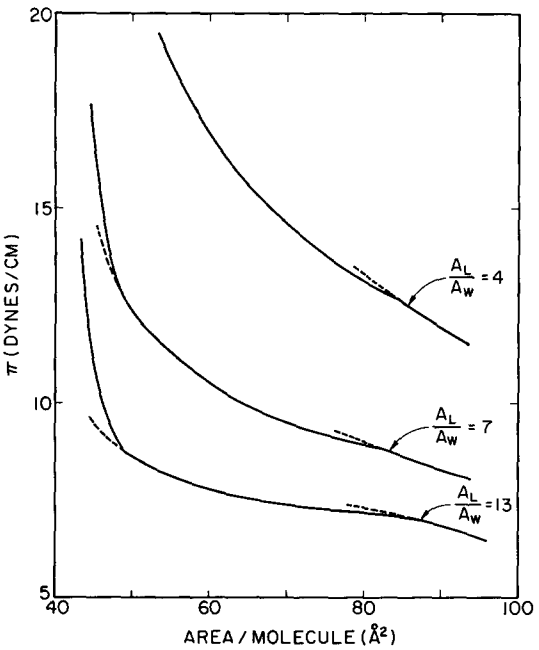

Fig. 5. Effects of different lipid head group cell size on the π/A isotherms at $T = 290$ °K. A_L/A_w is the ratio of the molecular surface area of lipid to that of the unbound water.

tacitly assume that the true long range cooperativity of the hydrocarbon chains is disrupted, perhaps by impurities, or perhaps by the dynamics of the head group-water surface itself. In any case, we then can, in a first approximation, treat the two pressure contributions independently. In Fig. 4 each of the two isotherms has two slope discontinuities, although they are not as distinct as those observed experimentally. The short dotted line segments illustrate the normal continuation of the curves. Because the isotherms in Fig. 4 are steeper than those observed experimentally, and the slope discontinuities less apparent, we have also performed the analysis described above for various values of the lipid head group cell size relative to the area per water molecule. In Fig. 5 we plot, for $T = 290$ °K, the resulting isotherms for values of

TABLE II

PROPERTIES OF THE HYDROCARBON CHAIN PHASE TRANSITIONS

Theoretical values include hydrocarbon chain contributions only. Areas in parentheses are experimental values from ref. 1.

		Area/molecule (Å²)		Entropy change (cal/mol per degree)	
T(° K)	A	Condensed	Expanded	Theory	Experiment [1]
290	29.0	53.5	85 (86)	3.4	38
294	28.6	50	76 (76)	6.8	66
299	28.1	48	65 (64)	8.7	84

A_L/A_w, the ratio of head group to water areas of 4 (same as in Fig. 4), 7, and 13. It is apparent that, for larger A_L/A_w the isotherms take on shapes which more closely resemble the experimental isotherms of ref. 1. In fact, one may compare qualitatively the isotherm for $A_L/A_w = 7$ to that of dipalmitoyl phosphatidylcholine at 17 °C (Fig. 3 of ref. 1) and the isotherm for $A_L/A_w = 13$ to that of dipalmitoyl phosphatidylethanolamine at 20 °C (Fig. 2 of ref. 1). The agreement is not as good in this latter case, as the condensation point in the experimental data is approx. 70 Å^2 as compared to 80 Å^2 for the theory. This is partly because the theoretical isotherm is calculated at only 17 °C. The $T = 294$ °K isotherm for the chains, which has a condensation point at 76 Å^2 (Table II) would provide a better fit, for large A_L/A_w, to the phosphatidylethanolamine data. We stress that perfect agreement between experiment and theory is not to be expected at this stage. The results we present here do not consider the details of the complex head group-water interactions, and thus should not be expected to perfectly reproduce experimental isotherms. Rather, we present a plausible molecular explanation of the observed behavior of some phospholipid monolayers.

(IV) RESULTS AND CONCLUSIONS

The properties of the model which result from hydrocarbon chain interactions are summarized in Table II. The entropy changes for this model are larger than those in our earlier calculations [10], but still much smaller than the experimental values. The obvious source of at least part of the discrepancy lies in the fact that the model considered only about 10^4 states (when the weight factors are included) whereas the estimated total number of states for a two chain model with 24 rotatable bonds is 10^{10} or 10^{11} (some isomeric states are sterically forbidden so 3^{24} is an overestimation). However, an increase by three orders of magnitude in the number of states has only resulted in roughly a 2-fold increase in ΔS. Therefore, it may be that surface contributions play an important part in the ΔS observed experimentally. In fact, contributions from the surface pressure can only produce a larger value for $d\pi_c/dT$, used by Phillips and Chapman in ref. 1 to calculate the entropy charges at the transition points (see Eqn 22 below). One other source of difference lies in the fact that the area per molecule in the condensed phase is taken as 47 Å^2 independently of temperature by Phillips and Chapman [1]. Certainly for the given data this is the most logical choice, but our model indicates A_s may be higher, although experimental detection of the slope discontinuities at higher π may be very difficult. The experimental transition heat is estimated by using the relation:

$$\frac{d\pi_c}{dT} = \frac{Q}{T(A_L - A_s)} \tag{22}$$

where π_c is the condensation pressure, A_L and A_s the molecular areas in the "liquid" and "solid" states respectively, Q the latent heat, and T the absolute temperature. Therefore, an increased value of $d\pi_c/dT$ as well as a decreased value of A_s over these attributable to a pure chain model will lead to larger estimates of ΔS. The true entropy changes for the hydrocarbon chains may therefore be lower than the values quoted in ref. 1. Still, we do expect the values listed in Table II are too low. Although the numerical techniques used in this work are faster and more accurate than those used in ref. 10, the number of states and layers are now near a practical upper limit. As

stated earlier [10] and confirmed by the calculations presented here, an increase in the number of allowed conformational states will not significantly alter the qualitative behavior of the model.

The primary results of this work are contained in Figs 4 and 5 which show the combined isotherms at $T = 290$ and 299 °K. All these isotherms have the same type of slope discontinuity as observed experimentally, with the discontinuity at larger A_L/A_w easiest to observe. As mentioned earlier, the method by which these discontinuities is obtained involves the assumption that the monolayer phase transitions are not perfect (in the sense of classical fluids) first-order phase changes. We speculate that the most likely source for this disruption of what is normally expected to be a first-order CH_2 chain melting is the head group-water interface. The surface tension of this interface must change continuously with changes in area per head group. Thus, the surface forces may impede any true cooperative change in the hydrocarbon region. In summary, the calculations indicate that when both hydrocarbon chain and head group-water contributions are included in a monolayer pressure calculation, the theoretical model reproduces the properties observed experimentally. We conclude that the experimental isotherms are not significantly in error due to surface impurities, and thus represent true monolayer behavior. In the phase transition between liquid-expanded and gaseous monolayers the experimental isotherms are flat. Within the context of our model, this may be due to the fact that, when this transition occurs, the monolayer is already so expanded that the surface pressure due to the head groups is very small. Then the hydrocarbon chains become the predominant source of pressure π and true cooperative behavior may be observed.

Another important result of this work is the theoretical demonstration that, when steric forces are considered, the kink states seem to form more easily than other states. This is true in this model even though a kink requires energy 2ε compared to ε for a single gauche rotation. We are, therefore, forced to conclude that models which consider only non-steric van der Waals interactions among the hydrocarbon chains cannot be considered to accurately represent all aspects of hydrocarbon chain cooperative behavior. In support of this claim we note that estimates of the melting entropy based on a free chain model [25] are too high unless a *trans*-gauche energy barrier of 1400 cal/mol rather than the experimental value of 500 cal/mol is used. When Belle et al. [26] estimate the effects of steric forces (by placing each chain in a hexagonal cell whose size varies with the average interchain distance) they obtain melting entropies in much closer agreement with experimental values.

It is natural to now consider the relationship between these results and the observed phase transitions in bilayer vesicles and membranes. The bilayer transitions resemble more closely liquid-solid melting than vapor-liquid condensation in that they occur only at single characteristic temperatures, very nearly independently of water pressure [27]. At the characteristic temperatures, calorimetry experiments reveal very sharp anomalies in specific heat [28]. The difference between monolayer and bilayer phase transitions is probably related to the freedom of movement of the head groups in the two situations. In bilayers, it seems that hydrophobic forces would constrain the head groups to align themselves fairly close together at all but very high temperatures to isolate the chains from water. The hydrophobic forces must reach a kind of dynamic equilibrium with the inter-head group repulsive forces and this restricts the density range available to the hydrocarbon chains. However, in monolayers the

chains are above the water surface and should find it energetically favorable to remain there even when polar head groups are very far apart. In fact, in the highly expanded gaseous monolayers, lipid chains may, in fact, come quite near the surface [7], but it is not likely that they penetrate it to any great extent. This extra degree of freedom available to monolayers can certainly produce different types of cooperative behavior of the systems involved. It seems, therefore, that in a successful theoretical analysis of bilayer phase transitions it may be possible to at least partially neglect the head group-water interactions and still retain a successful theory.

Finally, the deficiencies of the hydrocarbon chain model have been discussed elsewhere [10, 15] and the calculations of the head group pressure are admittedly crude and of limited validity. Nevertheless, the model presented here does provide a satisfactory explanation for monolayer phase transitions and, most importantly, points out the importance of the hydrophilic portion of the lipids in understanding lipid-water systems physically. A subsequent paper dealing with the effects of cholesterol on monolayer phase transitions is in preparation.

APPENDIX A

A list of the functions X $(\{\alpha_i\})$

$$
\begin{aligned}
X_0 &= 3+\alpha_1+2\alpha_2+3\alpha_3+4\alpha_4+5\alpha_5+6\alpha_6+7\alpha_7+8\alpha_8+9\alpha_9+2\alpha_{10} \\
&\quad +3\alpha_{11}+2\alpha_{12}+3\alpha_{13}+4\alpha_{14}+5\alpha_{15}+\alpha_{16}+2\alpha_{17}+3\alpha_{18}+4\alpha_{19}+5\alpha_{20} \\
X_1 &= 3+\alpha_1+\alpha_2+2\alpha_3+3\alpha_4+4\alpha_5+5\alpha_6+6\alpha_7+7\alpha_8+8\alpha_9+2\alpha_{10}+2\alpha_{11}+2\alpha_{12} \\
&\quad +2\alpha_{13}+3\alpha_{14}+4\alpha_{15}+\alpha_{16}+2\alpha_{17}+2\alpha_{18}+3\alpha_{19}+4\alpha_{20} \\
X_2 &= 3+2\alpha_2+\alpha_3+2\alpha_4+3\alpha_5+4\alpha_6+5\alpha_7+6\alpha_8+7\alpha_9+\alpha_{10}+2\alpha_{11}+\alpha_{12}+2\alpha_{13} \\
&\quad +2\alpha_{14}+3\alpha_{15}+\alpha_{16}+2\alpha_{17}+3\alpha_{18}+4\alpha_{19}+3\alpha_{20} \\
X_3 &= 3+3\alpha_3+\alpha_4+2\alpha_5+3\alpha_6+4\alpha_7+5\alpha_8+6\alpha_9+\alpha_{12}+2\alpha_{13}+3\alpha_{14} \\
&\quad +4\alpha_{15}+\alpha_{16}+2\alpha_{17}+3\alpha_{18}+4\alpha_{19}+5\alpha_{20} \\
X_4 &= X_3+3\alpha_4-3\alpha_3-\alpha_5-\alpha_6-\alpha_7-\alpha_8-\alpha_9 \\
X_5 &= X_4+4\alpha_5-4\alpha_4-\alpha_6-\alpha_7-\alpha_8-\alpha_9 \\
X_6 &= X_5+5\alpha_6-5\alpha_5-\alpha_7-\alpha_8-\alpha_9 \\
X_7 &= X_6+6\alpha_7-6\alpha_6-\alpha_8-\alpha_9 \\
X_8 &= X_7+7\alpha_8-7\alpha_7-\alpha_9 \\
X_9 &= X_8+8\alpha_9-8\alpha_8
\end{aligned}
$$

APPENDIX B

Derivation of Eqn 6 [19]

In general, the Helmholtz free energy of a mixture has the form

$$
\mathrm{d}F = -S\,\mathrm{d}T - p\,\mathrm{d}V + \sigma\,\mathrm{d}A + \sum_i \mu_i\,\mathrm{d}n_i \tag{B1}
$$

where S is the entropy, T the absolute temperature, p the pressure, V the volume, σ the surface tension, A the surface area, and μ_i and n_i the chemical potential and number of particles for species i. In the "monolayer model" of a surface one assumes the surface is a well-defined single layer one molecule thick. If this is the case, then

$$A = \sum_i a_i n_i^{(s)} \tag{B2}$$
$$dA = \sum_i a_i dn_i^{(s)}$$

where a_i is the area per molecule of species i and $n_i^{(s)}$ the number of type i molecules in the surface. Then the chemical potential is not a simple derivative of F with respect to n_i, but

$$\left(\frac{\partial F}{\partial n_i^s}\right)_{T,\ldots} = \mu_{i_m}^s + \sigma a_i \tag{B3}$$

The subscript m denotes the fact that this is the chemical potential in the monolayer model.

Now Defay et al. [19] make use of the general thermodynamic relation

$$\left(\frac{\partial F}{\partial n_i^s}\right)_{T,\ldots} = \mu_i^s = \mu_i^{s,o} + \boldsymbol{k}T \ln (x_i^s \gamma_i^s) \tag{B4}$$

where $\mu_i^{s,o}$ is the chemical potential for species i in an ideal mixture. The second equality makes use of the definition of the activity coefficient γ_i, and x_i^s is the concentration of species i in the surface. Equating the expression from the monolayer model, B3, to the general expression B4 yields

$$\mu_{i_m}^s + \sigma a_i = \mu_i^{s,o} + \boldsymbol{k}T \ln (x_i^s \gamma_i^s), \tag{B5}$$

or

$$(\mu_{i_m}^s - \mu_i^{s,o}) = \boldsymbol{k}T \ln (x_i^s \gamma_i^s) - \sigma a_i \tag{B6}$$

Now in Eqn B6 let $x_i^s \to 1$. Then $\sigma \to \sigma$ (pure) and $\gamma_i^s \to \gamma_i^s$ (pure). The surface tension and activity coefficient for a pure surface of species i then obeys the equation

$$(\mu_{i_m} - \mu_i^o)^s = \boldsymbol{k}T \ln (\gamma_i^s(\text{pure})) - \sigma(\text{pure}) a_i \tag{B7}$$

In the above equations we have assumed that a_i, the area per molecule, is unchanged as x_i changes. Now assume that species i is the sole constituent of the substrate (bulk) and any other members of the mixture are confined to the plane monolayer surface. Then, in equilibrium,

$$\mu_{i_m}^s = \mu_i^B \tag{B8}$$

where μ_i^B is the bulk chemical potential which is, for practical purposes, independent of x_i^s, the concentration of substrate molecules in the surface. Then in both Eqns B6 and B7 we may replace μ_i^s by μ_i^B and then, since μ_i is a constant, we may equate the right hand sides to obtain

$$(\sigma(\text{pure}) - \sigma) = -\frac{\boldsymbol{k}T}{a_i} \ln (x_i^s \gamma_i^s / \gamma_i^{s,p}). \tag{B9}$$

But the left hand side of the above equation is the surface pressure in the monolayer model, so that

$$\pi = -\frac{\boldsymbol{k}T}{a} \ln (x \gamma_R) \tag{B10}$$

where we have dropped the obvious subscripts and defined the relative activity coefficient:

$$\gamma_R = \gamma_i^s/\gamma_i^{s,p} \tag{B11}$$

This is Eqn 6 of the paper. Eqn B10 is similar to a result obtained by a different method by Fowkes [29].

APPENDIX C

The activity coefficient in statistical mechanics

We begin with the Grand Canonical Partition Function for a single component classical system

$$\Xi(T, V, \mu) = \sum_{N=0}^{\infty} \frac{e^{\beta\mu N}}{N!} Z_N(T, V) \tag{C1}$$

where $\beta = 1/\boldsymbol{k}T$, μ is the chemical potential and Z_N is the Canonical Partition Function, given for a classical system by

$$Z_N(T, V) = \frac{1}{h^{3N}} \int dp_1 - dp_N \exp\left(-\sum_i p_i^2/2m\boldsymbol{k}T\right) \int_V dr_i - d\bar{r}_n \exp\left(-\sum_{i<j} v(r_{ij})/\boldsymbol{k}T\right) \tag{C2}$$

The quantity $v(r_{ij})$ is the interparticle pair potential. One normally writes Eqn C3 in the form

$$Z_N(T, V) = f^{3N}(T) Q_N(V, T) \tag{C3}$$

where

$$Q_N(V, T) = \int_V dr_1 \ldots dr_n \exp\left(-\sum_{i<j} v(r_{ij})/\boldsymbol{k}T\right) \tag{C4}$$

For an ideal gas, $v(r_{ij}) = 0$ so that $Q_N(V) = V^N$. Thus, we define

$$q_N(V, T) = \frac{Q_N(V, T)}{V^N} \tag{C5}$$

Then Eqn C3 becomes

$$Z_N(T, V) = f(T)^{3N} V^N q_N(V, T) \tag{C6}$$

Now in general when fluctuations are small one finds the terms in the sum in Eqn 1 are all very much smaller than one particular term, namely that N which corresponds to the average $N = \bar{N}$ [25]. Thus, we may write

$$\Xi(T, V, \mu) \cong \frac{e^{\beta\mu\bar{N}}}{\bar{N}!} Z_{\bar{N}}(T, V) \tag{C7}$$

where $\bar{N}$ satisfies

$$(\partial/\partial N \ln \Xi)_{N=\bar{N}} = 0 \tag{C8}$$

as well as a second criterion that the second derivative be negative, which becomes a thermodynamic stability statement.

Substituting Eqn C6 into Eqn C1 and performing the differentiation indicated in Eqn C8 we obtain an equation for $\mu(T,\bar{N})$

$$-\mu/\boldsymbol{k}T = -\partial/\partial N \ln(N!)+3 \ln f(T)+\ln V+\partial/\partial N \ln q_N(V,T) \tag{C9}$$

Now in an ideal gas all the terms except the last one on the right are present (this can easily be verified by explicitly evaluating Ξ for an ideal gas and differentiating with respect to μ to obtain $\bar{N}(\mu,V,T)$, then inverting to obtain $\mu(T,V,N)$). Therefore, we write

$$\mu = \mu \text{ (ideal)}+\boldsymbol{k}T \ln a \tag{C10}$$

where, by definition,

$$\ln a = -\partial/\partial N \ln q_N (V,T). \tag{C11}$$

The extension of the above calculation to a binary mixture is straightforward. The Grand Partition function for the mixture can be written as

$$\Xi(T, V, \mu_1, \mu_2) = \sum_{N_1, N_2} e^{\beta(\mu_1 N_1 + \mu_2 N_2)}/N_1!N_2!Z_{N_1,N_2}(T, V) \tag{C12}$$

We evaluate this expression by applying maximum term arguments to each of the two sums to obtain

$$\mu_i = \mu_i(\text{ideal})-\boldsymbol{k}T\partial/\partial N_i \ln q_{N_1,N_2} \tag{C13}$$

Therefore, the activity coefficient defined by Eqn 7 in the text is given by

$$\ln x_i\gamma_i = -\boldsymbol{k}T\partial/\partial N_i \ln q_{N_1,N_2} \tag{C14}$$

This is Eqn 8.

ACKNOWLEDGEMENTS

We are grateful to C. Tanford, C. T. Butler and S. Marčelja for helpful discussions, to J. F. Nagle and S. Marčelja for preprints of their work prior to publication and to J. Belle for informing us of ref. 26. Part of the numerical analysis was performed using the subroutine MARQ written by L. W. Jackson and J. P. Chandler, Computer Science Department, Oklahoma State University. Portions of this work were supported by National Science Foundation Grant No. BMS 74-12731.

REFERENCES

1 Phillips, M. C. and Chapman, D. (1968) Biochim. Biophys. Acta 163, 301–313, and references contained therein.
2 Tanford, C. (1974) J. Phys. Chem. 78, 2469–2479
3 Adam, N. K. (1941) The Physics and Chemistry of Surfaces, Chapter II, Oxford University Press, London
4 Gaines, G. L. (1966) Insoluble Monolayers at the Liquid Gas Interface, John Wiley and Sons, New York

5 Gershfeld, N. F. and Pagano, R. E. (1972) J. Phys. Chem. 76, 1231–1237
6 Nagle, J. F. (1973) J. Chem. Phys. 58, 252–264
7 Nagle, J. F. (1975) J. Chem. Phys. 63, 1255–1261
8 Marčelja, S. (1974) Biochim. Biophys. Acta 367, 165–176
9 Marčelja, S. (1974) J. Chem Phys. 60, 3599–3604
10 Scott, H. L. (1975) J. Chem. Phys. 62, 1347–1355
11 Seelig, J. (1974) Biochemistry 13, 1585–1588
12 Shih, C. S. and Alben, R. H. (1972) J. Chem. Phys. 57, 3056–3061
13 Alben, R. (1971) Mol. Cryst. Liq. Cryst. 13, 193–229
14 Flory, P. J. (1956) Proc. R. Soc. London, Ser. A, 234, 60–73
15 Nagle, J. F. (1974) Proc. R. Soc. London, Ser. A, 337, 569–589
16 Straley, J. P. (1973) Mol. Cryst. Liq. Cryst. 22, 333–357
17 Onsager, L. (1947) Ann. N.Y. Acad. Sci. 51, 627–659
18 Gershfeld, N. (1968) Adv. Chem. Ser. 84, 115–130
19 Defay, R., Prigogine, I., Bellemans, A. and Everett, D. H. (1966) Surface Tension and Adsorption, pp. 210–211, John Wiley and Sons, New York
20 Prigogine, I. and Defay, R. (1954) Chemical Thermodynamics, p. 88, Longmans, London
21 Chapman, P., Williams, R. M. and LadBrooke, B. D. (1967) Chem Phys. Lipids 1, 445–475
22 Gaines, G. L. (1966) Insoluble Monolayers at the Liquid Gas Interface, p.256, John Wiley and Sons, New York
23 Defay, R., Prigogine, I., Bellemans, A. and Everett, D. H. (1966) Surface Tension and Adsorption, p. 257, John Wiley and Sons, New York
24 Gupta, S. P. and Govil, G. (1972) FEBS Lett. 27, 68–70
25 Bothorel, P., Belle, J. and Lemaire, B. (1974) Chem. Phys. Lipids 12, 96–116
26 Belle, J., Bothorel, P. and Lemaire, B. (1974) FEBS Lett. 39, 115–117
27 Srinivasan, S. R., Kay, R. L. and Nagle, J. F. (1974) Biochemistry 13, 3494–3496
28 Hinz, H. S. and Sturtevant, J. M. (1972) J. Biol. Chem. 247, 6071–6075
29 Fowkes, F. M. (1962) J. Phys. Chem. 66, 385–390